

Epitaxial and highly electrical conductive La_{0.5}Sr_{0.5}TiO₃ films grown by pulsed laser deposition in vacuum

Wenbin Wu, Fei Lu, K. H. Wong, Geoffrey Pang, C. L. Choy et al.

Citation: *J. Appl. Phys.* **88**, 700 (2000); doi: 10.1063/1.373724

View online: <http://dx.doi.org/10.1063/1.373724>

View Table of Contents: <http://jap.aip.org/resource/1/JAPIAU/v88/i2>

Published by the [American Institute of Physics](#).

Related Articles

Surface rippling on bulk metallic glass under nanosecond pulse laser ablation

Appl. Phys. Lett. **99**, 191902 (2011)

Negative ions: The overlooked species in thin film growth by pulsed laser deposition

Appl. Phys. Lett. **99**, 191501 (2011)

High-frequency electromagnetic properties of epitaxial Bi₂FeCrO₆ thin films grown by pulsed laser deposition

Appl. Phys. Lett. **99**, 183505 (2011)

Al and Fe co-doped transparent conducting ZnO thin film for mediator-less biosensing application

AIP Advances **1**, 042112 (2011)

Effects of stress on the optical properties of epitaxial Nd-doped Sr_{0.5}Ba_{0.5}Nb₂O₆ films

AIP Advances **1**, 032172 (2011)

Additional information on J. Appl. Phys.

Journal Homepage: <http://jap.aip.org/>

Journal Information: http://jap.aip.org/about/about_the_journal

Top downloads: http://jap.aip.org/features/most_downloaded

Information for Authors: <http://jap.aip.org/authors>

ADVERTISEMENT

**AIPAdvances**

Submit Now

**Explore AIP's new
open-access journal**

- **Article-level metrics
now available**
- **Join the conversation!
Rate & comment on articles**

Epitaxial and highly electrical conductive $\text{La}_{0.5}\text{Sr}_{0.5}\text{TiO}_3$ films grown by pulsed laser deposition in vacuum

Wenbin Wu^{a)} and Fei Lu

Structure Research Laboratory, University of Science and Technology of China, Hefei 230026, China and Department of Applied Physics, The Hong Kong Polytechnic University, Kowloon, Hong Kong, China

K. H. Wong, Geoffrey Pang, and C. L. Choy

Department of Applied Physics and Materials Research Center, The Hong Kong Polytechnic University, Kowloon, Hong Kong, China

Yuheng Zhang

Structure Research Laboratory, University of Science and Technology of China, Hefei 230026, China

(Received 4 January 2000; accepted for publication 17 April 2000)

The target material with nominal composition of $\text{La}_{0.5}\text{Sr}_{0.5}\text{TiO}_3$ sintered in air is an insulator and not a single-phase compound. By pulsed laser ablation in vacuum at the multiphase La–Sr–Ti–O target, however, highly electrical conductive and epitaxial $\text{La}_{0.5}\text{Sr}_{0.5}\text{TiO}_3$ films have been fabricated on $\text{LaAlO}_3(001)$ substrates. Structural characterization using three-axis x-ray diffraction (θ – 2θ scan, ω -scan rocking curve, and ϕ scan) reveals that the films have a pseudocubic structure and grow on the substrates with a parallel epitaxial relationship. Atomic force microscopy images show the films have quite smooth surface, for a film 200 nm thick, the roughness R_a is about 0.31 nm over the $1\ \mu\text{m}\times 1\ \mu\text{m}$ area. Resistivity versus temperature measurements indicate that the films are metallic at 2–300 K and have resistivity of $64\ \mu\Omega\ \text{cm}$ at 300 K, which is about one order lower than that of the single-phase $\text{La}_{0.5}\text{Sr}_{0.5}\text{TiO}_3$ bulk materials. After the same deposition procedure, epitaxial $\text{La}_{0.5}\text{Sr}_{0.5}\text{TiO}_3$ films have also been grown on TiN buffered (001) Si substrates. © 2000 American Institute of Physics. [S0021-8979(00)07014-6]

I. INTRODUCTION

The family of perovskite oxides displays a broad range of technologically important phenomena, including superconductivity, magnetism, and ferroelectricity. Due to the underlying structural and chemical similarities of these materials, and because of recent advances in their vapor deposition in thin film form, it is now possible to take advantage of such diverse behavior in epitaxial heterostructures. Epitaxial and highly electrical conductive perovskite-type oxide films have been found useful for electrodes and junctions in such heterostructures for oxide electronic devices.^{1–4} An example of these structures was $\text{La}_{0.5}\text{Sr}_{0.5}\text{CoO}_3$ /ferroelectric/ $\text{La}_{0.5}\text{Sr}_{0.5}\text{CoO}_3$, for ferroelectric nonvolatile memory cells. Over the past several years, the metallic conductive $\text{La}_{0.5}\text{Sr}_{0.5}\text{CoO}_3$, LaNiO_3 , SrRuO_3 , and $\text{La}_{0.7}\text{Sr}_{0.3}\text{MnO}_3$ thin films and related epitaxial heterostructures have been extensively studied.^{3–11} When properly doped, $\text{La}_{1-x}\text{Sr}_x\text{TiO}_3$, a relatively newly synthesized solid solution system, also shows metallic conductivity at room temperature.^{12–14} Tokura and co-authors have investigated the filling (x) dependence of the metallic properties on the verge of the Mott–Hubbard transition in $\text{La}_{1-x}\text{Sr}_x\text{TiO}_3$ bulk materials.¹² Surely, fabrication of epitaxial $\text{La}_{1-x}\text{Sr}_x\text{TiO}_3$ thin films will be important for both basic scientific research and actual applications. However, to our knowledge, the growth of epitaxial $\text{La}_{1-x}\text{Sr}_x\text{TiO}_3$ (except for $x=1$) films has not been reported yet.

On the other hand, the epitaxial all-perovskite heterostructures usually need to be grown on silicon substrates to realize their applications in microelectronics. For the integration, buffer layer(s) will be inserted between the Si and the multilayered oxide system due to structural, thermal, and chemical mismatches between them.^{10,15–18} Until now, there are few reports on epitaxial growth of perovskite-type oxide films directly onto the Si wafer. In general, a prerequisite of growing an epitaxial film on Si is that the film could be deposited in a reduced or inert-gas atmosphere to avoid oxidizing the surface of the Si wafer at the deposition temperature.^{16–18} As has been reported by several groups, single-phase $\text{La}_{1-x}\text{Sr}_x\text{TiO}_3$ compounds could be synthesized only in reduced atmosphere,^{12,14} indicating the possibility to grow $\text{La}_{1-x}\text{Sr}_x\text{TiO}_3$ directly onto Si substrates. In this article, we try to grow $\text{La}_{0.5}\text{Sr}_{0.5}\text{TiO}_3$ (LSTO) on the lattice-matched single crystal LaAlO_3 (LAO) substrates first. Our results will demonstrate that by pulsed laser deposition (PLD) in the vacuum atmosphere, epitaxial and highly electrical conductive LSTO films of perovskite-like structure could be grown on the LAO and TiN buffered Si substrates.

II. EXPERIMENT

The target used for PLD of the LSTO films was made by conventional solid state reactions in air with starting materials La_2O_3 (99.9% purity), SrCO_3 (99.5% purity), and TiO_2 (99.99% purity). The nominal composition was $\text{La}_{0.5}\text{Sr}_{0.5}\text{TiO}_3$. The sintering temperature was 1200–1300 °C, and during the target preparation, grinding, press,

^{a)}Electronic mail: wuwb@ustc.edu.cn

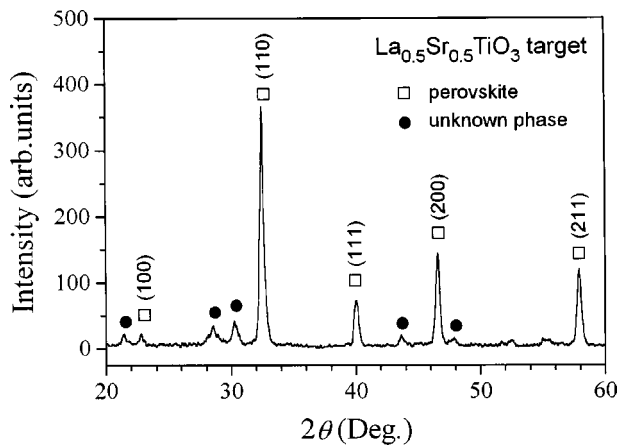


FIG. 1. XRD pattern of the target air-sintered from the mixture of stoichiometrical $\text{La}_{0.5}\text{Sr}_{0.5}\text{TiO}_3$ composition.

and sintering were repeated three times. The LSTO films were fabricated on LAO(001) (perovskite subcell indices) or the TiN buffered Si (001) substrates by PLD for 15 min, using KrF excimer laser ($\lambda=248$ nm, Lambda Physik, Complex 205) of 10 Hz in repetition frequency. The laser energy density irradiated on the rotating target was 4 J/cm^2 . The target-substrate distance was 45 mm. Before the deposition the chamber was evacuated by a cryopump to a base pressure of 5×10^{-7} Torr, the growth temperature was $550\text{--}700$ °C and during deposition the chamber pressure was 2×10^{-6} Torr. After deposition the films were cooled also at the base pressure. The thickness of the LSTO films is about 200 nm.

X-ray diffraction (XRD) patterns were obtained with $\text{Cu } K\alpha$ radiation (Ni filter) by a four-circle diffractometer. Scanning electron microscopy and atomic force microscopy (AFM) operated in air at room temperature were employed to characterize the surface morphology of the films. A standard four-probe method was used to measure the resistivity of the films between 2 and 300 K. X-ray photoemission spectra (XPS) were taken by using a monochromatized x-ray source of $\text{Mg } K\alpha$ radiation ($h\nu=1253.6$ eV) and the energy resolution was about 0.8 eV.

III. RESULTS AND DISCUSSION

Figure 1 shows the XRD pattern of the air-sintered La–Sr–Ti–O target. It is seen that the target is not a single-phase compound. Apart from reflections that could be indexed according to a pseudocubic perovskite phase, some reflections from other unknown phase(s) appeared. Because in air atmosphere the most stable oxide of the titanium is TiO_2 with Ti^{4+} , when replacing the Sr^{2+} by the La^{3+} , a reduced ambient is usually indispensable to decrease the Ti valence state from +4.0.^{12–14} The resistivity of the target material at room temperature is larger than $10^8 \Omega \text{ cm}$.

To create a reduced atmosphere for the growth of stoichiometric $\text{La}_{0.5}\text{Sr}_{0.5}\text{TiO}_3$ (LSTO) compound, we made use of the multiphase target and the vacuum atmosphere (2×10^{-6} Torr) to deposit LSTO films by the PLD method. Figure 2 shows XRD patterns of a typical LSTO film deposited at 650 °C. Although the target is not of single phase, no impurity phases were recorded for the as-deposited film. In

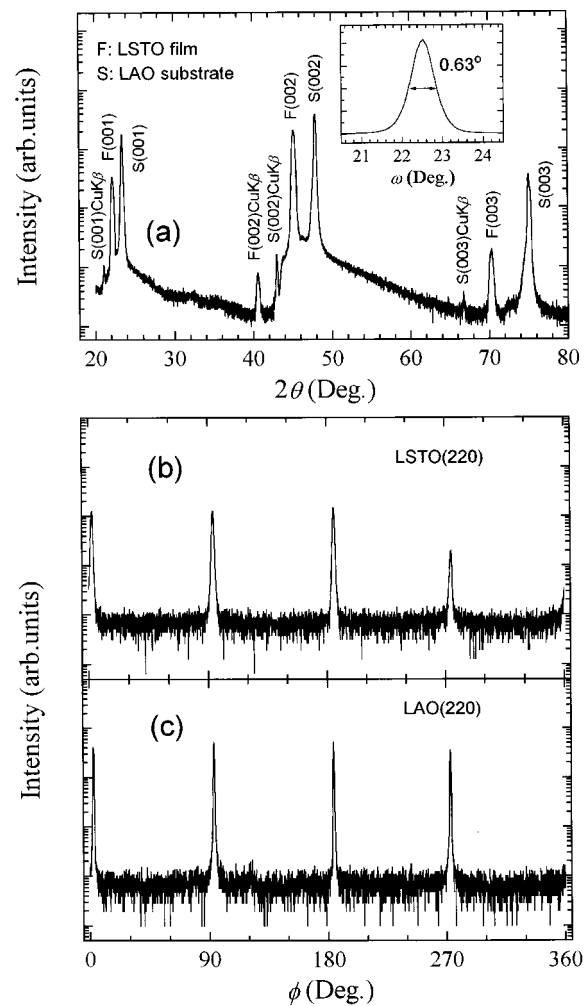


FIG. 2. XRD patterns of LSTO/LAO(001) heterostructures deposited at the base pressure of 2×10^{-6} Torr. (a) The XRD linear scan from the LSTO/LAO(001) and the inset shows the rocking curve on the LSTO(002) reflection. In (b) and (c), XRD ϕ scans on the LSTO(220) and LAO(220) reflections are shown, respectively.

Fig. 2(a), strong reflections from LSTO(001) diffraction planes appeared and were indexed according to a pseudocubic structure. Some weak peaks due to the $\text{Cu } K\beta$ radiation were also indexed. The inset shows the XRD rocking curve on the LSTO(002) reflection. The full width at half maximum (FWHM) of the curve is 0.63° , indicating good crystalline quality of the film. Note that the FWHM of the rocking curve on the LAO(002) reflection is 0.31° . Figures 2(b) and 2(c) show x-ray ϕ scans on the LSTO(220) and LAO(220) reflections of the LSTO/LAO(001) heterostructure, respectively. A good in-plane epitaxy is evidenced. It is clear that at the vacuum ambient single-crystalline LSTO films have been grown on the LAO(001) substrates and the epitaxial relationship is $[100]\text{LSTO}(001)/[100]\text{LAO}(001)$.

The surface of the LSTO films grown at the vacuum atmosphere is very smooth. Scanning electron microscopy images show no features of the film surface even with a magnification of 10^5 (not shown). Figure 3(a) shows a typical AFM image taken for the same LSTO film shown in Fig. 2. The roughness R_a over the $1 \mu\text{m} \times 1 \mu\text{m}$ surface is only 0.31 nm. Some of this roughness is attributable to the pres-

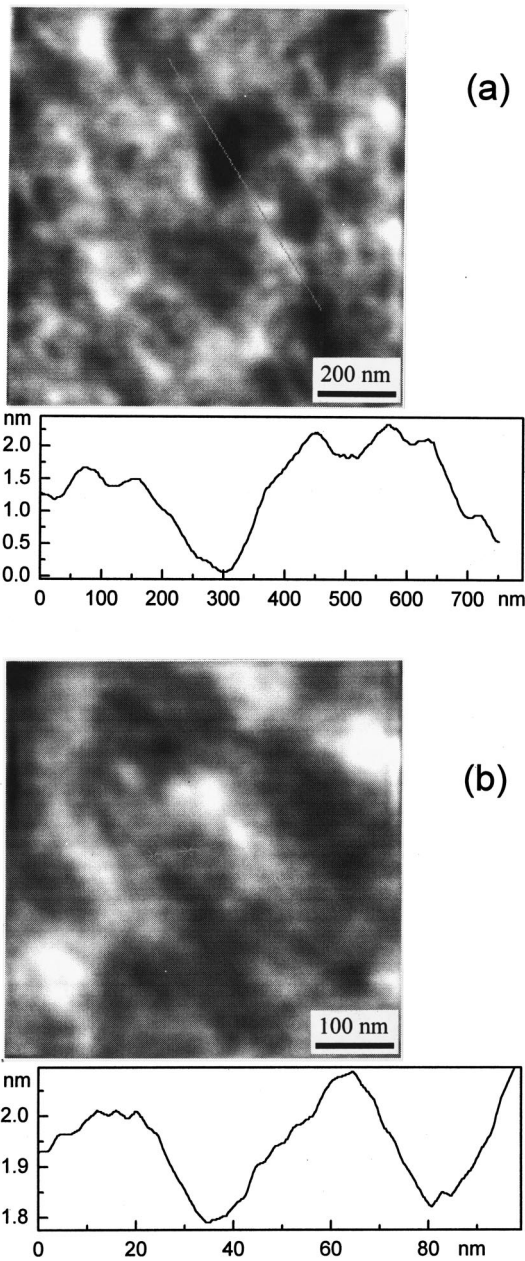


FIG. 3. Typical AFM images of the LSTO film on LAO(001) substrates. In (a) and (b) the dark area and steps of about one unit height were scanned, respectively.

ence of a few voids with about 200 nm in diameter and 1.8 nm in depth, as reflected by the line scan across the dark area in the image. From the line scan analysis of the image (the area is $0.5 \mu\text{m} \times 0.5 \mu\text{m}$) shown in Fig. 3(b), steps with height of about just one lattice unit length (4.03 \AA) were also recorded. At present, the low roughness observed for the epitaxial LSTO films is not clearly understood. In general, it is believed that at reduced oxygen pressures laser–solid interactions produce species with energies large enough to damage the solid surfaces upon which they impinge.¹⁹ For a material system that could be grown in vacuum ambient such as the LSTO, the case may be quite different.

Figure 4 shows the normalized Ti_{2p} and O_{1s} (the inset) spectra from the epitaxial LSTO film (solid line) and the

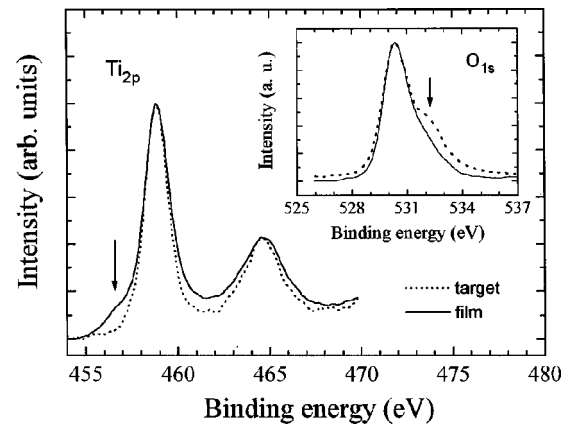


FIG. 4. Core-level spectra of the Ti_{2p} and O_{1s} (the inset) from as-grown LSTO films (solid line) and the target material (dashed line).

target material (dashed line). Compared with the target material, the absorbate (O atom) intensity in the O_{1s} spectrum from the film is significantly reduced, as denoted by the arrow. For the Ti_{2p} spectrum, apart from the peak at 458.85 eV, which is usually attributed to the atoms with Ti^{4+} , a new component at a lower binding energy of 456.6 eV appeared. These spectra clearly reflect that the valence-state and chemical environment of the Ti atom in the films and the target material are different. The composition of the epitaxial LSTO films was also checked by the XPS measurements and the ratio of La:Sr:Ti was 0.44:0.56:1.02, near the nominal ratio of the target.

Figure 5 shows the temperature dependence of resistivity measured for the epitaxial LSTO films grown at 650°C . A metallic transport behavior was observed over the whole temperature range of 20–300 K. The resistivity at room temperature was about $64 \mu\Omega\text{cm}$, which is about one order lower than that of the single-phase $\text{La}_{1-x}\text{Sr}_x\text{TiO}_3$ ($x=0.5$) bulk materials.¹² Tokura *et al.* found that for bulk LSTO, the temperature dependence of resistivity could fit well by the $\rho = \rho_0 + AT^2$ relation and they described the transport behavior by the Fermi liquid model.¹² For the epitaxial LSTO film, the resistivity–temperature profile was found fit well by $\rho = \rho_0 + AT^{2.5}$ at higher temperatures, as shown in the inset. At temperatures lower than 150 K, however, the relation does

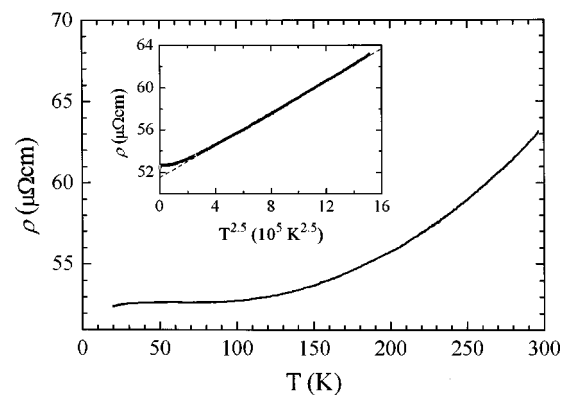


FIG. 5. The temperature dependence of resistivity measured for the LSTO film grown at 650°C . The inset shows dependence of the resistivity on $T^{2.5}$.

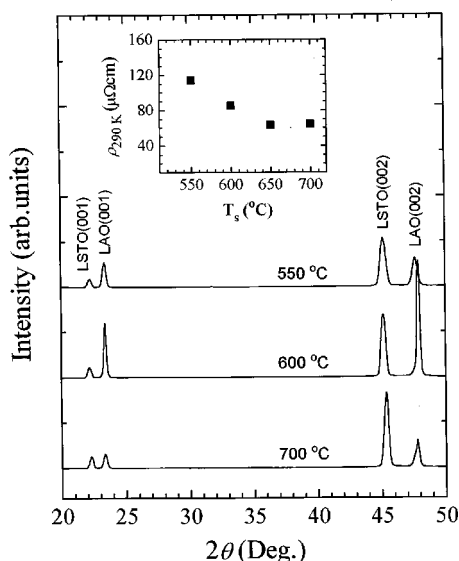


FIG. 6. XRD patterns of LSTO films grown at 550, 600, and 700 °C on the LAO(001) substrates. The inset shows dependence of the resistivity at room temperature on the deposition temperature.

not hold and the reduced temperature dependence is reminiscent of the resistivity-temperature profile of the superconducting $\text{La}_{1-x}\text{Sr}_x\text{TiO}_3$ single crystals.²⁰ The variation in the power suggests that there are at least two scattering mechanisms for the epitaxial LSTO films. With the temperature further decreasing, it is noted that the resistivity drops fast again. We have measured the resistivity at lower temperatures and found that although the resistivity decreased steadily, the films showed no superconductivity down to 2 K.

The growth of epitaxial LSTO films on LAO in vacuum (2×10^{-6} Torr) was studied at the deposition temperature range of 550–700 °C. Figure 6 shows XRD linear scans of the LSTO films deposited at 550, 600, and 700 °C, respectively. It was found that the LSTO film could be grown epitaxially at a low substrate temperature (T_s) of 550 °C. With the T_s increasing, the FWHM of the LSTO(00 l) ($l=1$ and 2) reflections is decreased, indicative of improved crystallinity of the films. In the inset, resistivity at 290 K of the epitaxial LSTO films was plotted against the T_s . With the T_s increasing, the resistivity at room temperature is decreased, which suggests that the conductivity is related to the crystallinity of the films.

Following the same deposition procedure, it was found that LSTO films could be grown epitaxially on the TiN buffered Si(001) substrates. With the use of a commercial hot-pressed TiN target, the TiN layer was deposited by PLD also at vacuum of 2×10^{-6} Torr, as described previously.¹⁶ Both the LSTO and TiN layers were grown *in situ* at 650 °C. Figure 7 shows the XRD linear scan of the LSTO/TiN/Si(001) heterostructure. Only LSTO(00 l) ($l=1$ and 2), TiN(002), and reflections of the Si(001) substrates were recorded. A cube-on-cube epitaxial relationship was also confirmed by x-ray off-specular linear scans and ϕ scans of the heterostructure. The inset to Fig. 7 shows a ϕ scan on the LSTO(220) reflection of the same heterostructure. The epitaxial relationship of the heterostructure is $[100]\text{LSTO}(001)/$

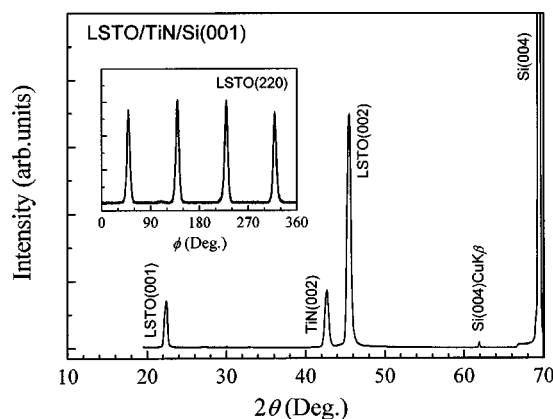


FIG. 7. XRD linear scan of a LSTO/TiN/Si(001) heterostructure. The inset shows the ϕ scan on the LSTO(220) reflection of the same heterostructure.

$[100]\text{TiN}(001)/[100]\text{Si}(100)$. The growth of LSTO films directly onto the Si(001) substrates is currently underway.

IV. CONCLUSIONS

In summary, epitaxial and highly electrical conductive LSTO films have been fabricated on LAO(001) substrates by PLD at vacuum of 2×10^{-6} Torr. Three-axis XRD and AFM studies indicate that the as-grown LSTO films have excellent structural and surface properties. The epitaxial LSTO films show a metallic transport behavior at 2–300 K and a low resistivity of $64 \mu\Omega \text{ cm}$ at room temperature. These films could be employed for both basic scientific research and the fabrication of all-perovskite heterostructures for actual applications. The PLD procedure and the target preparation process used in this work may also be applicable to deposit thin films of other oxide materials that need to be synthesized in reduced atmosphere, such as the La–Sr–V–O system.

ACKNOWLEDGMENTS

The work described in this article was supported by the Chinese Natural Science Foundation and a grant from the Research Grants Council of the Hong Kong Special Administrative Region (Project No. PolyU5160/98P).

- ¹R. Ramesh, A. Inam, W. K. Chan, B. Wilkens, K. Myers, K. Remschmig, D. L. Hart, and J. M. Tarascon, *Science* **252**, 944 (1991).
- ²M. Kasai, Y. Kanke, T. Ohno, and Y. Kozono, *J. Appl. Phys.* **72**, 5344 (1992).
- ³C. B. Eom, R. B. Van Dover, Julia M. Phillips, D. J. Werder, J. H. Marshall, C. H. Chen, R. J. Cava, R. M. Fleming, and D. K. Fork, *Appl. Phys. Lett.* **63**, 2570 (1993).
- ⁴J. Lee and R. Ramesh, *Appl. Phys. Lett.* **68**, 484 (1996).
- ⁵M.-S. Chen, T.-B. Wu, and J.-M. Wu, *Appl. Phys. Lett.* **68**, 1430 (1996).
- ⁶J. T. Cheung, P. E. D. Morgan, D. H. Lowndes, X. Y. Zheng, and J. Breen, *Appl. Phys. Lett.* **62**, 2045 (1993).
- ⁷R. A. Rao, Q. Gan, and C. B. Eom, *Appl. Phys. Lett.* **71**, 1171 (1997).
- ⁸X. D. Wu, S. R. Foltyn, R. C. Dye, Y. Coulter, and R. E. Muenchausen, *Appl. Phys. Lett.* **62**, 2434 (1993).
- ⁹Z. W. Dong, R. Ramesh, T. Venkatesan, M. Johnson, Z. Y. Chen, S. P. Pai, V. Talyansky, R. P. Sharma, R. Shreekala, C. J. Lobb, and R. L. Greene, *Appl. Phys. Lett.* **71**, 1718 (1997).
- ¹⁰Z. Trajanovic, C. Kwon, M. C. Robson, K.-C. Kim, M. Rajeswari, R. Ramesh, T. Venkatesan, S. E. Lofland, S. M. Bhagat, and D. Fork, *Appl. Phys. Lett.* **69**, 1005 (1996).
- ¹¹J. Z. Sun, W. J. Gallagher, P. R. Duncombe, L. Krusin-Elbaum,

- R. A. Altman, A. Gupta, Y. Lu, G. Q. Gong, and G. Xiao, *Appl. Phys. Lett.* **69**, 3266 (1996).
- ¹²Y. Tokura, Y. Taguchi, Y. Okada, Y. Fujishima, T. Arima, K. Kumagai, and Y. Iye, *Phys. Rev. Lett.* **70**, 2126 (1993).
- ¹³K. Kumagai, T. Suzuki, Y. Taguchi, Y. Okada, Y. Fujishima, and Y. Tokura, *Phys. Rev. B* **48**, 7636 (1993).
- ¹⁴M. Onoda and M. Kohno, *J. Phys.: Condens. Matter* **10**, 1003 (1998).
- ¹⁵B. Yang, S. Aggarwal, A. M. Dhote, T. K. Song, R. Ramesh, and J. S. Lee, *Appl. Phys. Lett.* **71**, 356 (1997).
- ¹⁶R. D. Vispute, J. Narayan, K. Dovidenko, K. Jagannadham, N. Parikh, A. Suvkhanov, and J. D. Budai, *J. Appl. Phys.* **80**, 6720 (1996).
- ¹⁷D. K. Fork, D. B. Fenner, G. A. N. Connell, J. M. Phillips, and T. H. Geballe, *Appl. Phys. Lett.* **57**, 1137 (1990).
- ¹⁸N. Tanase, K. Sano, K. Abe, and T. Kawakubo, *Jpn. J. Appl. Phys., Part 2* **37**, L151 (1998).
- ¹⁹J. P. Maria, S. Trolier-McKinstry, D. G. Schlom, M. E. Hawley, and G. W. Brown, *J. Appl. Phys.* **83**, 4373 (1998).
- ²⁰H. Suzuki, H. Bando, Y. Ootuka, I. Inoue, T. Yamamoto, K. Takahashi, and Y. Nishihara, *J. Phys. Soc. Jpn.* **65**, 1529 (1996).